Journal of Computer-Aided Molecular Design, 8 (1994) 491–512
ESCOM

J-CAMD 264

Derivation of a 3D pharmacophore model for the angiotensin-II site one receptor

Kristine Prendergast[a,*], Kym Adams[a], William J. Greenlee[b], Robert B. Nachbar[a], Arthur A. Patchett[b] and Dennis J. Underwood[a]

[a]*Molecular Systems Department and* [b]*Department of Exploratory Chemistry, Merck Research Laboratories, P.O. Box 2000, Rahway, NJ 07065, U.S.A.*

Received 18 November 1993
Accepted 20 May 1994

Key words: Computer-aided design; CoMFA; Conformational generation; Pharmacophore mapping; Systematic search

SUMMARY

A systematic search has been used to derive a hypothesis for the receptor-bound conformation of A-II antagonists at the AT_1 receptor. The validity of the pharmacophore hypothesis has been tested using CoMFA, which included 50 diverse A-II antagonists, spanning four orders of magnitude in activity. The resulting cross-validated R^2 of 0.64 (conventional R^2 of 0.76) is indicative of a good predictive model of activity, and has been used to estimate potency for a variety of non-peptidyl antagonists. The structural model for the non-peptide has been compared with respect to the natural substrate, A-II, by generating peptide to non-peptide overlays.

INTRODUCTION

Angiotensin-II (A-II) is an octapeptide hormone which possesses potent vasoconstrictor properties [1]. Peptidyl antagonists of the angiotensin-II site one (AT_1) receptor have indicated that blockade of this receptor site could provide an alternate route to modulating the activity of the renin–angiotensin system [2]. Recently, non-peptide A-II antagonists have been reported in the literature [3], and several show promise in the treatment of hypertension and congestive heart failure [4].

A knowledge of the three-dimensional (3D) structural requirements of the AT_1 receptor would provide an advantageous starting point for rational design of new A-II antagonists as well as helping to understand the existing structure–activity relationships (SARs). In this study, we present our model for the 3D receptor-bound geometry of A-II non-peptide antagonists, and provide evidence that it is consistent with the SARs for these compounds. Future work will

*To whom correspondence should be addressed.

illustrate the convergence of this model for the active conformation of bound antagonists with an independently derived model of the human AT_1 receptor, where the complementarity of chemical elements can be seen [5].

The crux of the problem is identifying which of the many conformations of a particular antagonist binds to the receptor, thereby blocking the effects of A-II. More generally, we would like to know whether it is possible to model the bioactive conformation of a ligand in the absence of explicit knowledge of the 3D structure of its receptor. Our approach to answer these questions begins with the work of Marshall [6] on ACE inhibitors; however, we have extended the validation process to include a CoMFA analysis [7] of the resulting hypothesis. A recent publication provides a clear example of the power of coupling these two approaches for use in drug discovery and design [8].

It is worthwhile to highlight the assumptions and limitations inherent in these techniques which may effect the outcome. Initially, a postulate of the pharmacophore was necessary. For our purposes, a pharmacophore is defined as a set of atoms or groups of atoms which, when presented in a well-defined 3D way, result in a biological response. This definition is, in general, one of an agonist pharmacophore. In consideration of binding of antagonists to a receptor, the definition would be adapted such that the 'biological response' is blockage of action of the agonist. Previously derived structure–activity relationships have identified *at least* three regions which are critical to AT_1 antagonism, and can be used to describe the *minimal* pharmacophore [9]. Referring

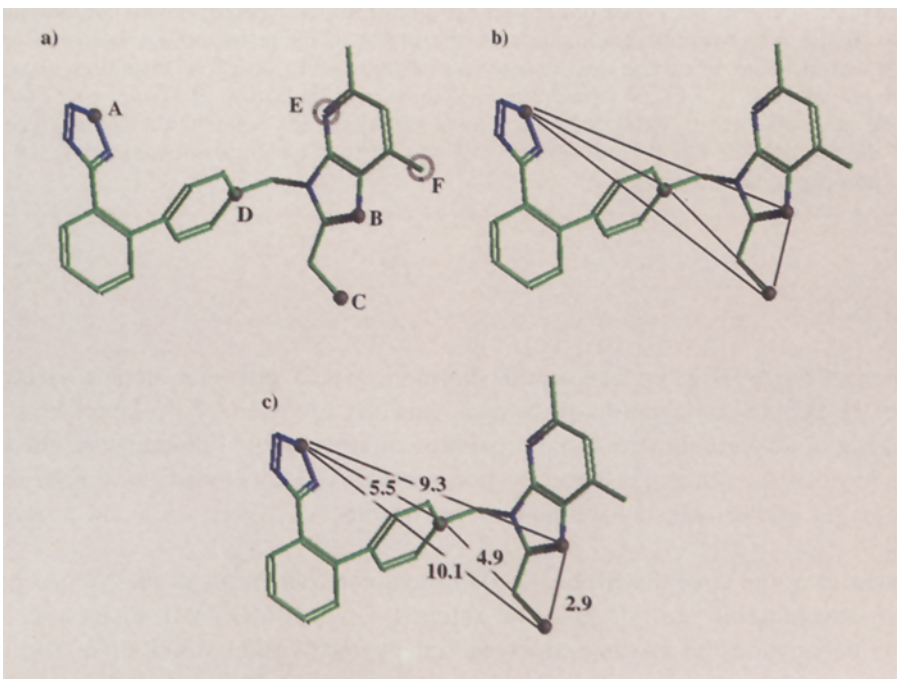

Fig. 1. (a) Illustration of the A-II pharmacophore model used in systematic search. The pharmacophore points are represented as gray spheres on the atomic centers of L-158809. (b) Distances used to define the A-II pharmacophore and monitored during search, illustrated on L-158809. (c) Final distances located by systematic search (in Å), illustrated on L-158809.

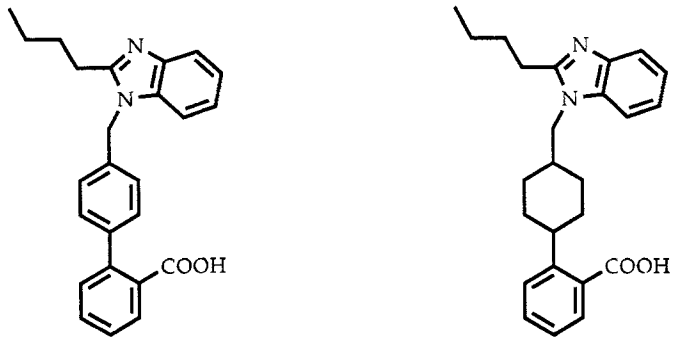

1a **1b**

Fig. 2. Structures of **1a** (0.5–0.65 μM) and **1b** (6.6 μM).

to Fig. 1a, these are: an acid group (**A**), an aromatic N (functioning as an H-bond acceptor) (**B**), and an alkyl side chain (**C**). The alkyl group must minimally be an ethyl group for a compound to exhibit AT_1 antagonism. A supplementary point in the biphenyl spacer (**D**) was added to the pharmacophore definition to reflect our belief that these linker groups themselves are important to binding, by providing an aromatic recognition element for the receptor. This is consistent with the 10-fold boost in potency exhibited by phenyl versus cyclohexyl derivatives (Fig. 2: **1a** = 0.5–0.65 μM versus **1b** = 6.6 μM) [10]. These points constitute our working pharmacophoric model.

Our goal was to determine whether a common structural hypothesis could integrate the activity data across classes of A-II antagonists. Thus, all molecules used in mapping were *required* to have this identifiable pharmacophore, and correspondence between functional groups in different molecules was determined by analogy. Active analogs presumably present the same 3D arrangement of pharmacophoric points when bound to the receptor. Inactive or less active compounds may be unable to present the 3D pharmacophore, either due to some steric or electrostatic impediment or because they lack some of the pharmacophore's essential features. Therefore, molecules that were used in map construction were highly active (IC_{50} = 10 nM or better). In our case, five distances were chosen between the pharmacophore points (Fig. 1b) to describe this yet undetermined geometry. A sequential, systematic search [6,11] was used to find common mappings of these distances: the first molecule was searched to define all permissible values of the five distances identified above. The second compound was searched to find intersections within the distance map, which is termed the orientation map (OMAP), of the first compound. Analogs were folded into the study until the number of ways of presenting the pharmacophore was reduced to unity. The result is a putative geometry for the pharmacophore points when an antagonist binds to the AT_1 receptor (Fig. 1c).

How can we judge whether the results of this process present a reasonable structural hypothesis? Several criteria can be used to evaluate the model:

(1) All active compounds should be geometrically able to achieve the pharmacophore geometry.

(2) Active compounds should not require excessive strain energy to achieve the pharmacophore geometry.

(3) Inactives which appear to possess the pharmacophore elements should not be capable of attaining the 3D pharmacophore geometry for the reasons noted previously.

Implicit to these validation criteria is the assumption that any useful model should be able to discriminate between active and inactive compounds. The traditional route to understanding the predictive ability of a model derived from systematic search has consisted of qualitative tests with select active and inactive compounds, and perhaps constructing volume and/or electrostatic potential maps to illustrate the features of the receptor cavity [12].

We note that active-analog mapping describes a set of rules by which molecules can be superposed. This is a suitable basis for a more quantitative evaluation of the individual steric and electrostatic factors contributing to activity differences, using a method such as comparative molecular field analysis (CoMFA). For the A-II antagonists considered in this work, CoMFA was successful in explaining SAR features and in further validation of the structural model derived using the active-analog approach. From the resulting statistical correlations, predictions of activities of molecules outside the CoMFA training set have been made. The CoMFA fields reveal rough details of how the AT_1 receptor may present itself to ligands which bind to it.

METHODS

Molecules used in pharmacophore mapping are shown in Fig. 3 [13]. The set of common distances for each active antagonist was located by searching all rotatable bonds using the systematic search protocol implemented in the program SYBYL [11]. Several parameters are required in the searching procedure, and affect the resolution of the resultant map. Our grid size, which determines the resolution of the distance map, was set to 0.2 Å. All rotatable bonds affecting the disposition of the pharmacophore were searched in 10° increments, from 0° to 360°. Some exceptions are noted, i.e., rotatable bonds which do not lie on a connected path between pharmacophore points were searched using 30° increments. Knowledge of local symmetry and the preference for amide bonds to be nearly planar were imposed to improve computational efficiency by reducing the search from a full 360° range. Aromatic rings were moved as rigid bodies.

The only criterion which rejects conformers during searching is a nonbonded steric interaction, which was set to 95% of the van der Waals radius. No conformational energy is evaluated, nor is minimization allowed during the search. Thus, the results of a systematic search locate an orientation map (OMAP) of all *geometrically* reasonable conformers of antagonists which present the pharmacophore in the same spatial arrangement as other antagonists. Post-search evaluation of the energetic feasibility of conformers, identified as being interesting, was carried out using OPTIMOL (MM2X) [14] with an intramolecular dielectric of 50 D. Convergence criteria were set to 2×10^{-2} kcal/Å.

CoMFA [18] was initiated using the conformation identified by systematic search to superpose active and inactive molecules. Only one superposition is considered in generating a CoMFA. However, for each molecule there are several conformers which can be described by the final OMAP distances. For the CoMFA analysis, one conformer corresponding to the most extended form of the alkyl chain and following closely the conformation of L-158809 shown in Fig. 1c was selected. Each molecule was held fixed at this optimized receptor-bound geometry and 1 SCF of MNDO [19] was carried out to assign Mulliken partial charges. All molecules were assigned a formal charge of zero. Both active and inactive compounds are needed in the derivation of a CoMFA, since the model must be trained to discriminate features which contribute to potency.

Fifty compounds, covering four orders of magnitude in activity and representing a diverse set of A-II antagonists, have been incorporated into the analysis (Fig. 4) [20].

The criteria in selecting compounds for inclusion in a systematic search and CoMFA differ: for a systematic search, as many diverse compounds as possible should be included to permute the atomic connections between the pharmacophoric points. It is considered important in the solution of the problem to have highly unique actives, as novel substituent patterns may eliminate possible OMAP points through steric clashes. However, in CoMFA (as in any QSAR) many representatives of each class would have to be included for the analysis to be meaningful. In the extreme limit of complete sample diversity, each compound would be explanatory for its own

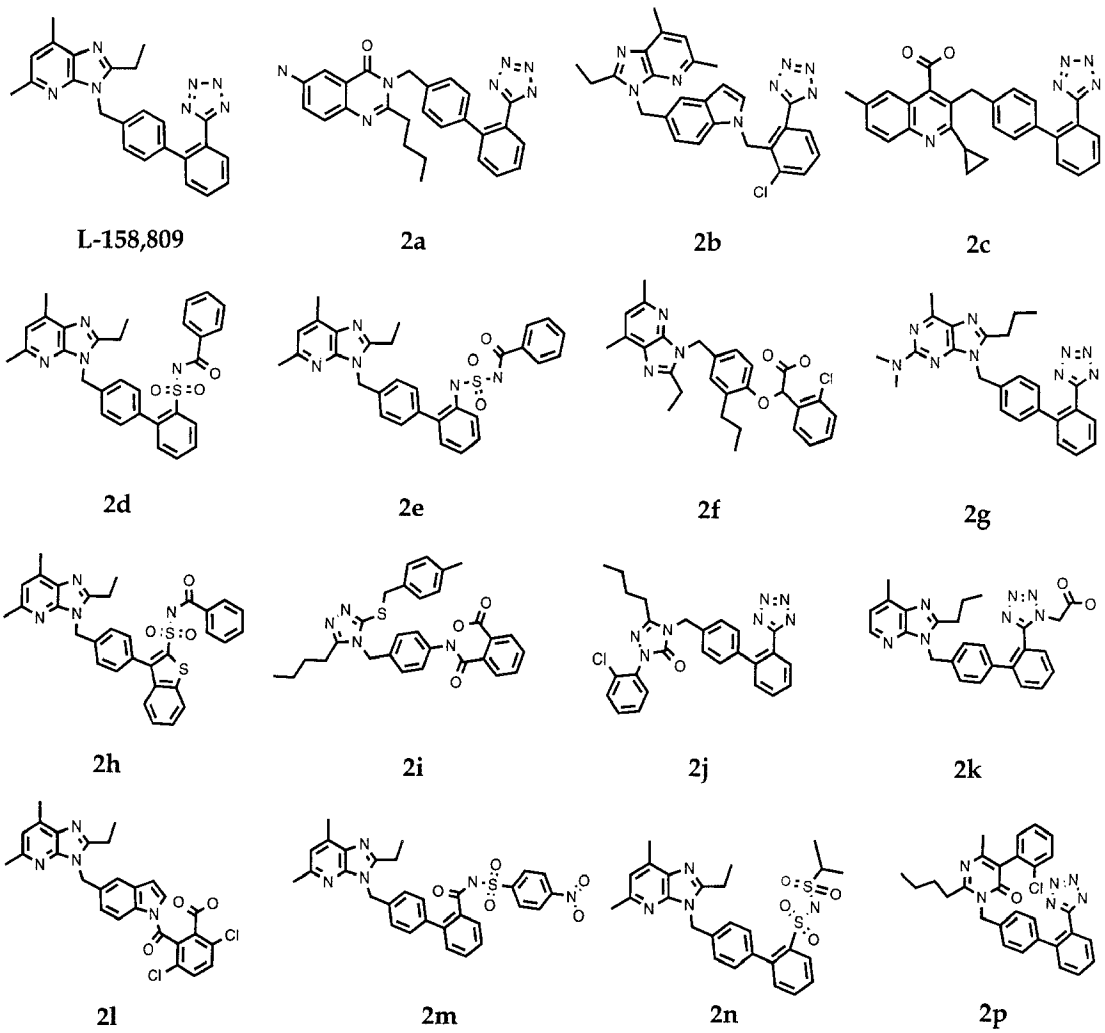

Fig. 3. Chemical structures of molecules used in systematic search. Since there is ambiguity in selection of the pharmacophore points, our selections are outlined: $\mathbf{C}_2$ of the alkyl chain on the heterocycle was always selected. The site of attachment of the acidic proton was selected (e.g., $\mathbf{N}_2$ site of the tetrazole, Ar-SO_2**N**HCO-X, Ar-SO_2**N**HSO_2-X, Ar-NHSO_2 **N**HCO-X, Ar-CONHSO_2-X, or Ar-COOH of a carboxylate). The –**N**= atom possessing an sp^2 lone pair adjacent to the alkyl group represents the hetero-atomic ring site, and the $\mathbf{C}_1$ position of the phenyl ring nearest to the hetero ring was used.

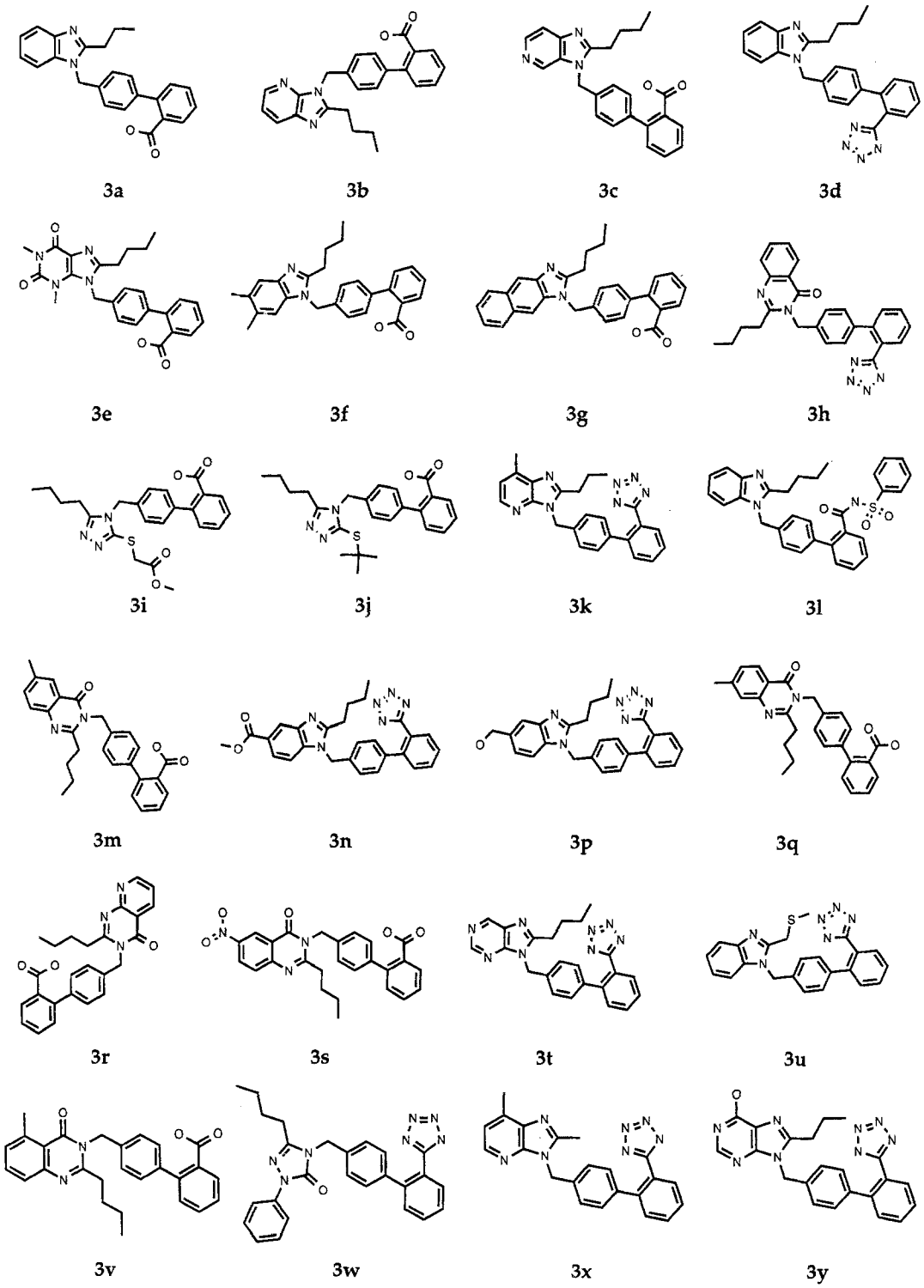

Fig. 4. Chemical structures of additional molecules used in the CoMFA training set and predictions (see Table 3).

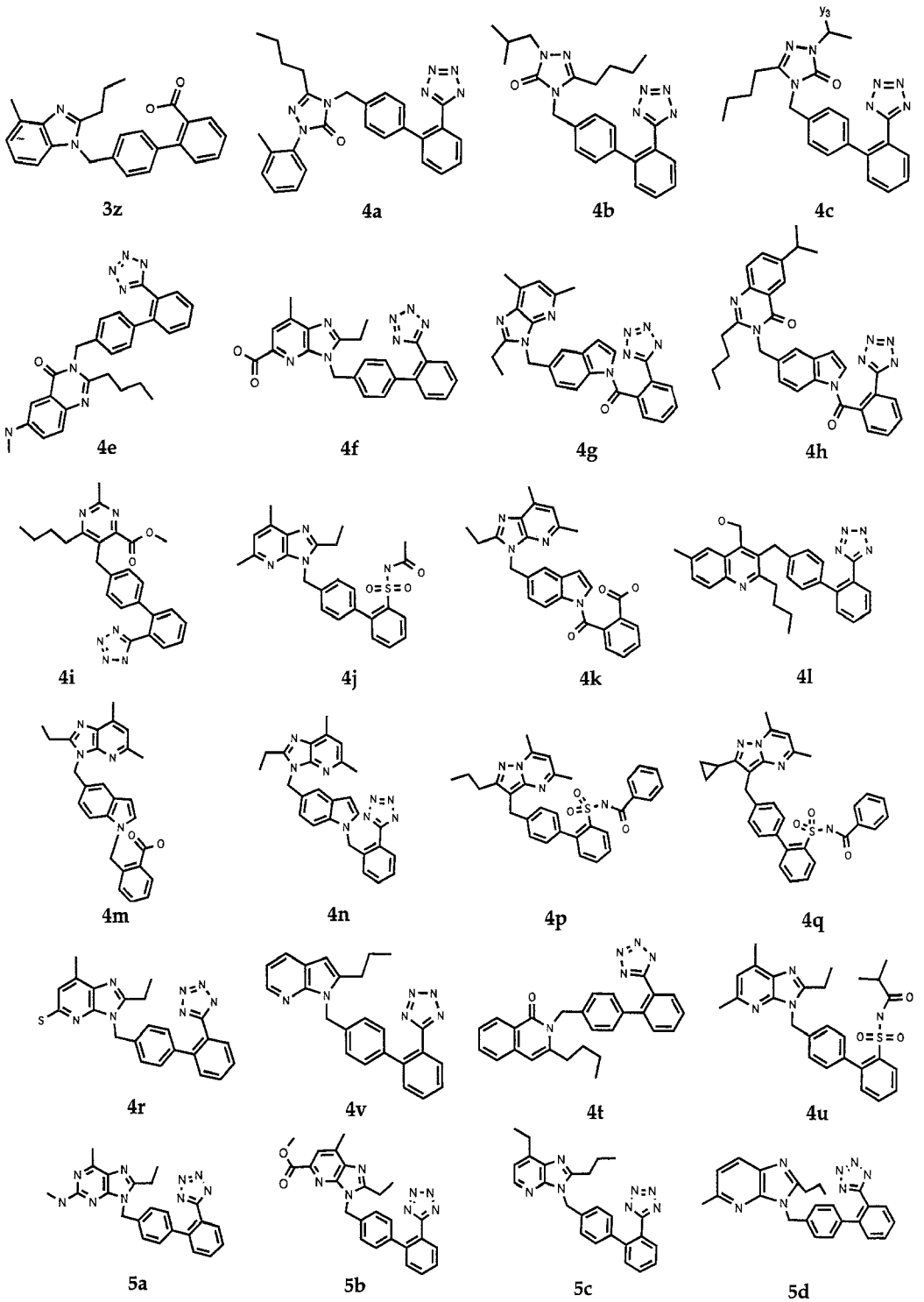

Fig. 4. (continued).

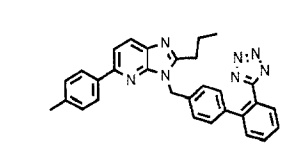

5e

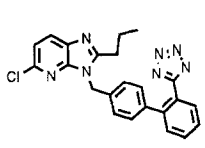

5f

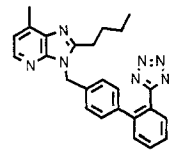

5g

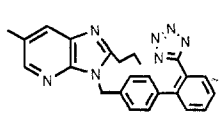

5h

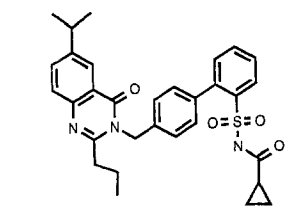

5i

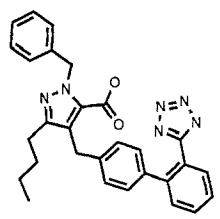

5j

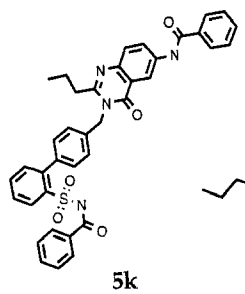

5k

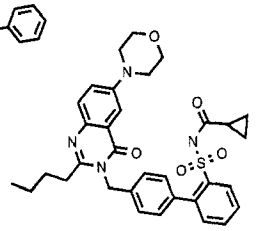

5l

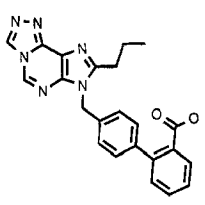

5m

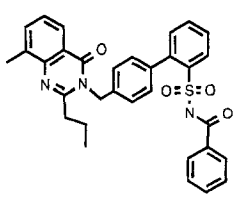

5n

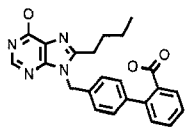

5p

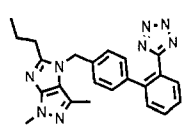

5q

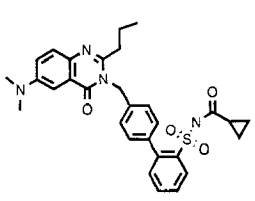

5r

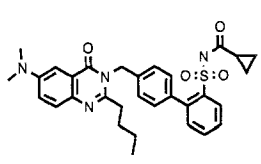

5s

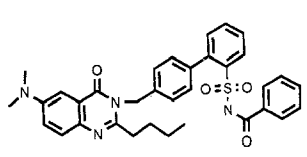

5t

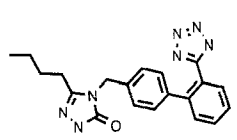

5u

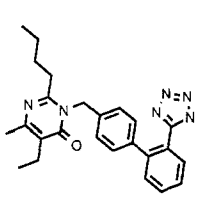

5v

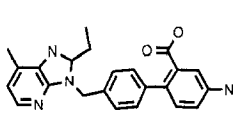

5w

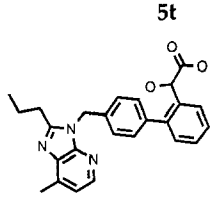

5x

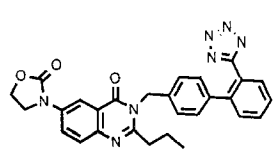

5y

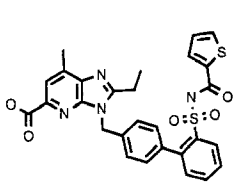

5z

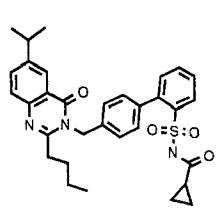

6a

Fig. 4. (continued).

TABLE 1
EFFECT OF CoMFA PARAMETERS ON R^2

	R^2	Components	F	Standard error
$\sigma = 2$				
5 cross-validation groups				
Full analysis	0.68	2	18.9	0.62
Steric only	0.61	3	13.8	0.70
Electrostatic only	0.59	2	12.4	0.71
50 cross-validation groups	0.64	2	42.3	0.66
0 cross-validation groups	0.75	2	69.6	0.56
$\sigma = 0$ [a]				
0 cross-validation groups	0.76	2	73.5	0.54

[a] The computational index was too large to complete the calculation at 50 cross-validation groups with $\sigma = 0$.

activity, a perfect correlation would occur, and the regression would have no predictive value because there is no relation between the compounds. Since several molecules in our systematic search spanned unique regions of property space which were not investigated fully, we limited our CoMFA analysis to structures with sufficient SARs to derive a reliable regression. We also did not include compounds from pharmacophore mapping which contained chlorine, because of known deficiencies in the steric parameters for halogens in the version of MAXIMIN2 that we used in constructing the CoMFA fields. Compounds close to these structures were included in the CoMFA analysis.

The pharmacophore points were aligned to generate a superposition, and points extraneous to the map were superposed as close as possible. The overlay of the entire array of rigid molecules was adjusted using SEAL [21], which combines atom-based steric and electrostatic factors with a Monte Carlo search procedure to refine the alignment of structures. The superposition used in deriving the CoMFA fields is shown in Fig. 5. Default CoMFA/PLS parameters of SYBYL 5.3 were selected, except that switching was turned on, and there was no volume averaging. Some optimization of CoMFA variables was attempted, and a partial summary of these studies is shown in Table 1. Not shown in Table 1 are the effects on how accurate a molecule must be aligned to correctly predict its activity in the given model: intentional misalignment of molecules being predicted shows that the alignment rules are of critical importance in generating reliable predictions. Misalignments in a particular coordinate direction have differential effects [22]. As a consequence of these findings, structures outside the training set were matched to a template from the CoMFA superposition which most closely resembled their structure. The compound was then optimized with the search constraints, and superposition to the template adjusted using SEAL with the MNDO charges. These alignments were used to evaluate the CoMFA field and predict activities from the final non-cross-validated analysis.

RESULTS AND DISCUSSION

The progress of the searching procedure is shown in Table 2. The choice of starting compound was based on the small number of rotatable bonds present in L-158809. The second compound,

TABLE 2
PROGRESS OF SYSTEMATIC SEARCH

Antagonist[a]	OMap points[b]	Rotatable bonds[c]	Strain energy[d]	Activity[e]	Reference
L-158809	12 750	5	0.3/0.0	0.2	13a
2a	793	7	0.6/0.2	5	13b
2b	546	6	0.7/0.4	2	13c
2c	301	6	0.6/0.1	9	13d
2d	78	8	2.6/3.5	0.1	13e
2e	78	9	7.6/1.0	0.1	13e
2f	55	9	1.4/2.1	8	13f
2g	48	7	0.4/0.0	3	13g
2h	32	7	4.1/2.6	2	13h
2i	31	12	0.4/0.2	7	13i
2j	31	8	2.4/0.0	2	13j
2k	31	8	0.3/0.1	8	13k
2l	5	6	0.8/0.4	3	13c
2m	4	8	0.8/4.6	0.2	13l
2n	4	8	3.4/1.0	0.6	16e
2p	1	8	0.6/0.1	2	13l

[a] Compounds are listed in order of inclusion into the systematic search analysis.
[b] Number of unique ways in which the defined pharmacophore can be presented at 0.2 Å resolution.
[c] Number of rotatable bonds scanned.
[d] Strain energy (kcal/mol) = (E(restrained at final OMap) – E(nearest minimum)). The first value has been calculated with MM2X [14], and the second entry has been calculated with MM2 [17].
[e] IC_{50} (nM) measured in rabbit aorta, and averaged from multiple evaluations.

2a, was required to match the distance ranges found when searching the space of L-158809. In this case, only 793 ways were common to the two. As the search proceeded, the number of common ways diminished. After the inclusion of 16 more compounds (Fig. 3), the unique ways in which the pharmacophore could be presented in *all* active antagonists was reduced to one (Fig. 1c).

For each molecule, there are several conformers which can be described by the final OMAP distances. Considering L-158809 as a representative example, relaxation using the MM2X force field with restraints of the final OMAP distances yields four distinct structures; two which differ by their intra-atomic coordinates and geometric isomers of each, which are generated by reflection through the heterocycle plane (Fig. 6). These four isomers are virtually degenerate in energy, which cannot be used to further discriminate between them. (Note that only four out of 12 750 initial conformers of L-158809 need to be considered with regard to the receptor-bound conformation when the final OMAP is imposed.) Other workers have attempted to describe the conformation of antagonists bound to A–II [23]. The conformation we chose to carry through the CoMFA analysis resembles the 'Helix 1' (H1) geometry with regard to the heterocycle–phenyl torsions [23d].

For active compounds, it is reasonable to assume that the strain energy to attain the binding orientation should be low. As shown in Table 2, strain energy is defined as the intramolecular energy above the nearest minimum. Energy was evaluated with both the MM2X [14,16] and MM2 [15,17] force fields using an intramolecular dielectric of 50 D. The energy was first calculated using the OMAP distances as restraints (0.2 Å bounds, 1 kcal/Å penalty for deviation from bounds). The restraints were then lifted and the energy was reevaluated. The difference in these

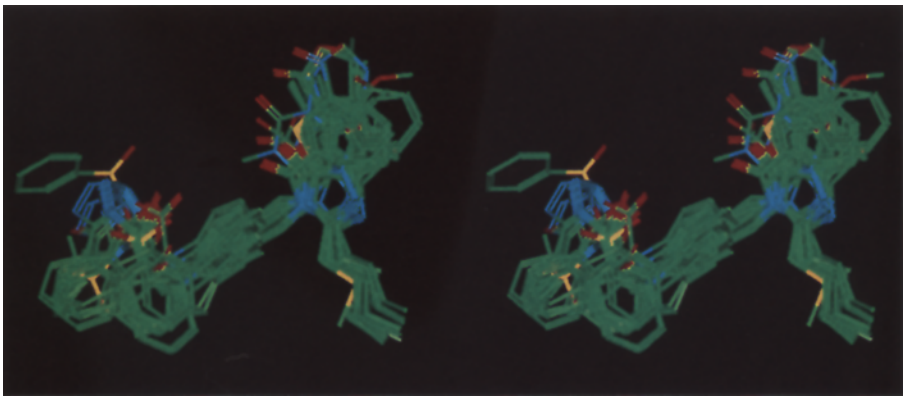

Fig. 5. Alignment of 50 molecules used in CoMFA after adjustment with SEAL.

terms was used as an indication of the strain energy, which for the most part was less than 4 kcal/mol (Table 2) for the 16 analogs used in deriving the OMAP. Much attention is given to locating the 'global' energy minima when deriving receptor maps [24]. The locations of global minima are highly dependent on details of the force field used and are expected to be sensitive to environmental factors such as the nature of the receptor. However, it is necessary to gain some insight into the position of the local minima relative to the lowest energy minimum within our

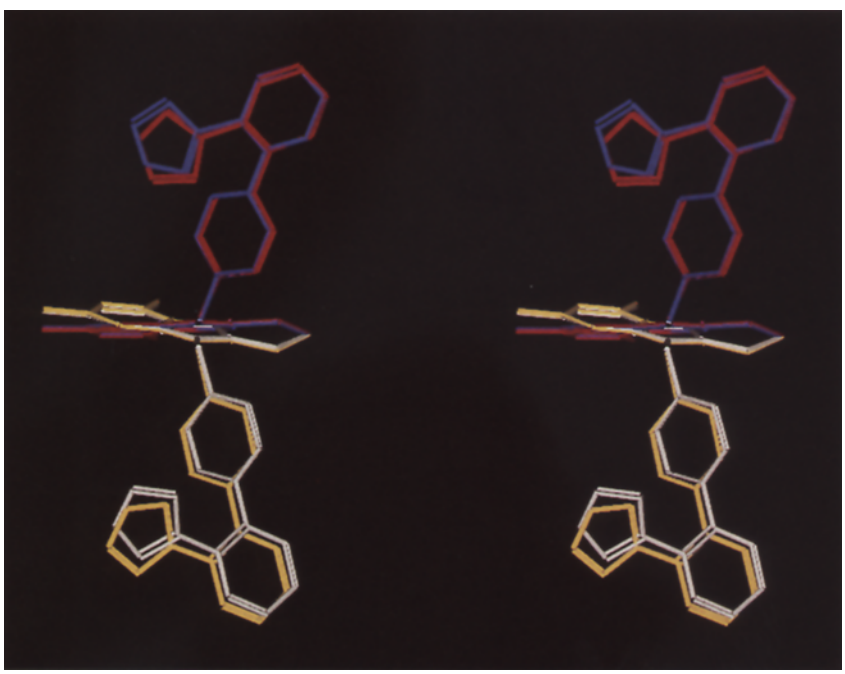

Fig. 6. The four energy-minimized 'isomers' of L-158809 which are consistent with OMAP distances. These structures are the result of geometry optimization of the conformers generated by systematic SEARCH. Conformer C (blue) was the nucleus for subsequent CoMFA analysis. Coordinates are available as supplementary material.

current model as described. Distance geometry methods (DGEOM) [25] and geometry optimization with MM2X were used to generate 500 conformers of each compound included in the search. Two compounds which bracket the range in minima located are L-158809, for which the energy of the bound conformer is less than 1 kcal/mol above the lowest energy structure located, and **2f**, where the bound conformation is 8 kcal/mol above the lowest located minimum. Thus, all compounds would fall in a 10 kcal/mol cutoff, which is generally accepted as reasonable in analyses of this sort. This range is realistic, given the approximations implicit in an empirical force field.

Based on these analyses, we concluded that the proposed structural model was energetically viable, and went on to gain insight into the requirements for activity. What makes a given compound active or inactive? Several possibilities exist. First, the compound may be unable to achieve the pharmacophoric pattern for reasons discussed above. Alternatively, it could lack some of the important pharmacophoric points. Finally, binding to the receptor could be either sterically or electrostatically compromised (or both). Thus, a working model should be able to account for features of inactivity as well as activity. Several compounds with a clear correspondence to our chosen pharmacophore were evaluated for their ability to attain the distance ranges depicted in Fig. 1c. While several relatively inactive compounds cannot attain the proposed pharmacophore geometry (CIBA6E, CIBA6D) [26], other inactives can (e.g. EX6155 [27], CIBA6A [26]) (Fig. 7). These findings indicate that there are more subtleties to activity differences than geometric fit to our 3D pharmacophore map.

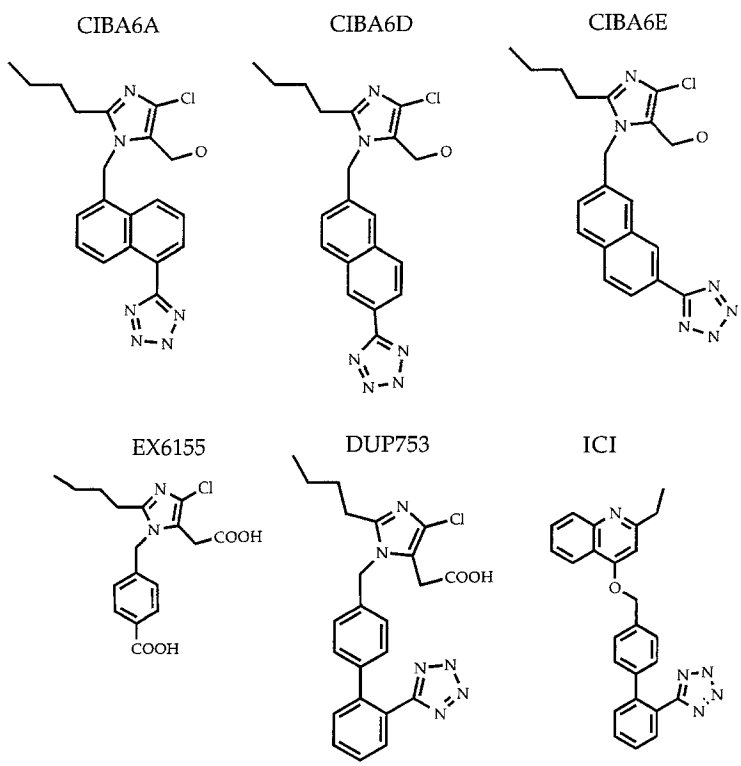

Fig. 7. Chemical structures of CIBA6A, CIBA6D, CIBA6E, EX6155, ICI and DUP753, as referenced in the text.

To help discern what these features are, we proceeded to develop a CoMFA model, also hoping that CoMFA could further validate our pharmacophoric pattern: if systematic search has located the bioactive arrangement of the pharmacophore points, we presume that statistically meaningful correlations and reasonable predictions of activities for molecules outside the training set would result.

The CoMFA yielded a predictive model of activity, which is characterized by a cross-validated R^2 of 0.64 and a conventional R^2 of 0.76. These values are somewhat surprising, given the wide range of compounds included in the study. This analysis used two components for optimal fitting, with a standard error in the cross-validated analysis of 0.662. Some of the fitted activities do deviate from their measured values (Table 3), but no outliers were removed from the analysis. Although this would undoubtedly improve the cross-validated R^2, there is no reason to expect any of the molecules contained in the training set to be incorrectly described. Thus, all were retained. For this same data set, steric only and electrostatic only runs were carried out, each yielding a slightly poorer correlation and predictive R^2, as noted in Table 1.

The penultimate test of a model is in its predictive power, purported to be reflected by the cross-validated R^2. In fact, the potential strength of CoMFA is that it could be used to prioritize synthetic targets by activity, or to identify and computationally screen novel scaffolds. We illustrate some examples of genuine predictions, made using our CoMFA model (see Fig. 8 and Table 3). The training set is heavy on traditional 'Merck' heterocycles; however, predictions on novel heterocyclic systems show the ability of the model to qualitatively rank which compounds may be of keenest interest. In accord with experiment, **5a** is predicted to be less active than both **5v** and **5q**, which are of similar potency. In addition, although no imidazoles were included in the training set, we were accurately able to predict the potency of DUP753 [28]. The correct estimation of the ICI compound [29] by our CoMFA analysis indicates that it falls within the spatial bounds of our analysis and does not sample any new property space, although this is not necess-

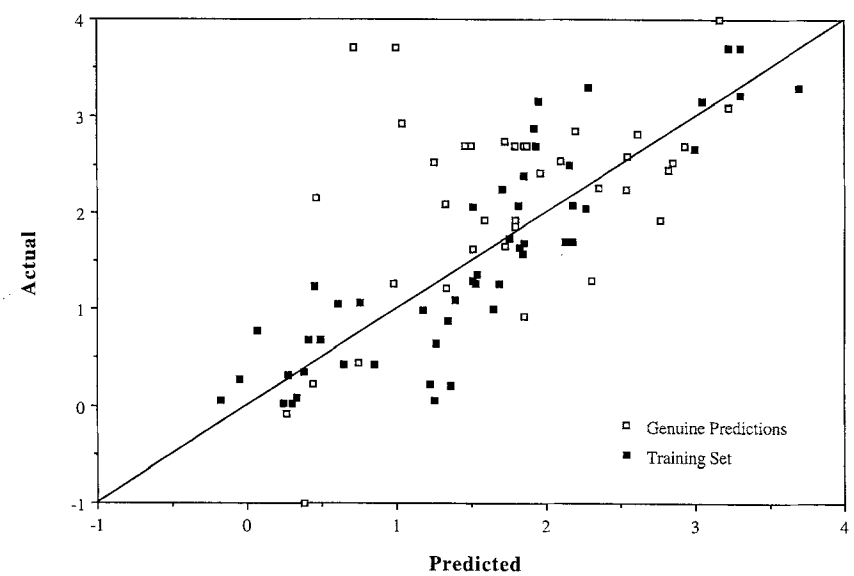

Fig. 8. Graph of predicted versus actual $-\log(IC_{50})$ as determined from the CoMFA analysis. The solid squares are molecules found in the training set and the open squares are molecules for which genuine predictions were carried out.

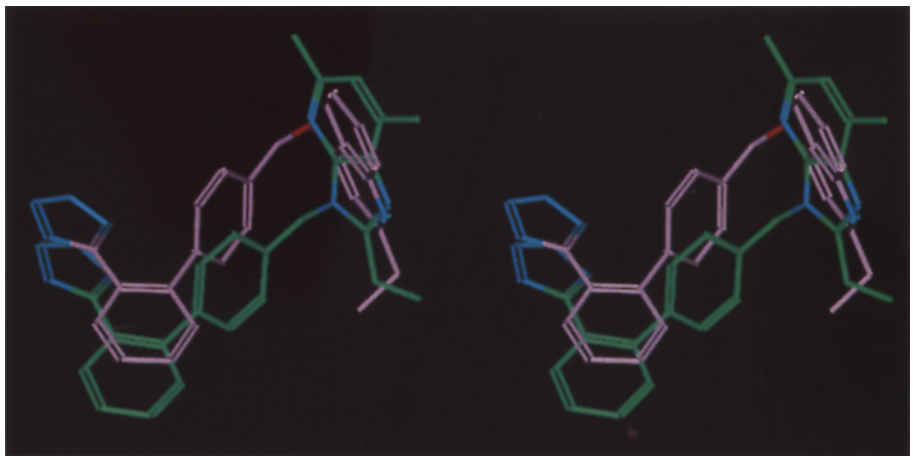

Fig. 9. Superposition of L-158809 and the ICI A-II antagonist which was used in making the CoMFA prediction of activity.

arily intuitive from a 2D perspective. The superposition used in the prediction of the ICI compound (Fig. 9) is consistent with functional group mappings identified previously [29]. However, the relative location of the tetrazole differs in our model.

It is clear from Table 3 that CoMFA can *generally* represent the activity of new compounds to within a log unit of their measured value, independent of whether they are active or inactive analogs. From the discussion above, one can identify select areas in which the qualitative trends can yield insight. To understand why a given prediction is likely to be correct or not, we attempted to correlate the residual ($IC_{50\ actual} - IC_{50\ predicted}$) with the topological similarity of the compound to the molecules of the training set. Using a joint similarity measure [30] to determine the distance of compound **A** to an average of all the molecules of the training set, no trends were visible: while each of the worst predictions had lower than average similarity to the training set (48% similar), some with the same similarity score were well described by the model. An alternative approach of judging the topological distance of each compound in the training set to each compound predicted in the analysis also failed to satisfactorily describe the observation. In some respects, it is gratifying that a 2D topological method is not capable of uncovering shortcomings of a 3D CoMFA analysis. However, a priori it is not obvious how well a given compound which seems to fall in the bounds of the analysis will be predicted, and we can offer no guidelines other than trial and error. In summary, the trends have proven to be generally true for our data set, but are not quantitatively accurate.

Does the CoMFA model make chemical sense based on what we know about A-II antagonism? An examination of the CoMFA fields (Fig. 10) tends to support the known SAR: CoMFA fields predict a steric wall for the alkyl site, beyond which added bulk will decrease potency. Placing electron-rich groups at the acid site is predicted to increase potency. It is noteworthy that CoMFA does not consider the original H-bond acceptor site or the phenyl rings in the biphenyl linker as adding to or detracting from activity. Most likely, this is due to the limited sampling of alternative functional groups in these regions. Other areas in the field maps can be perceived as important secondary pharmacophore points which affect the potency of an A-II antagonist,

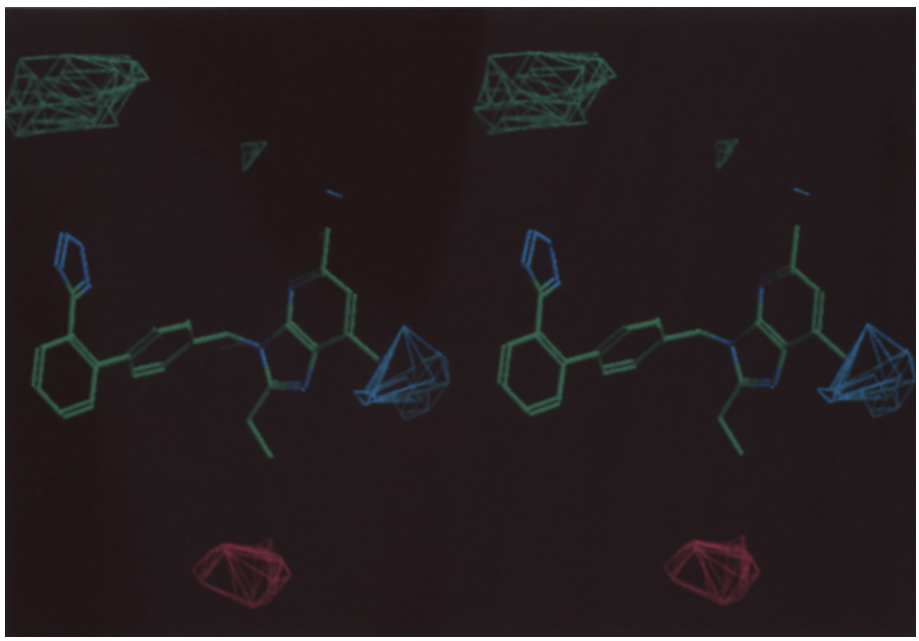

Fig. 10. Graphical representation of CoMFA fields. The fields were calculated as the product of the standard deviation and the coefficient to highlight those field points strongly associated with activity differences. Contours were drawn such that negatively charged (or proton acceptor) groups are favored where the contours are green. Red contours indicate a steric wall, while blue contours indicate sites which need bulk for optimum potency.

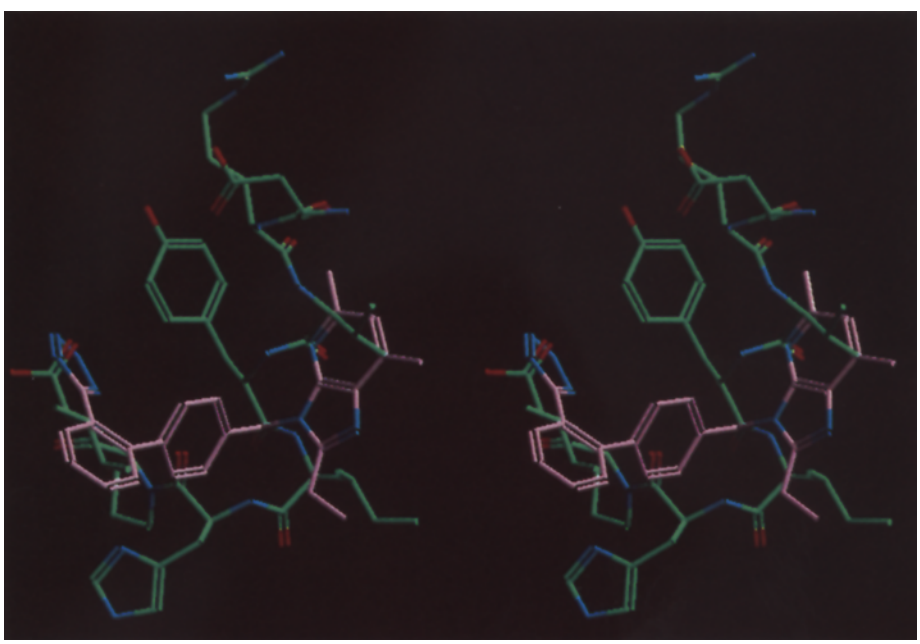

Fig. 11. An overlay between L-158809 and A-II, illustrating the proposed functional-group correspondence described in the text.

TABLE 3
PREDICTED AND EXPERIMENTAL ACTIVITIES FOR VARIOUS ANGIOTENSIN-II ANTAGONISTS

Training set activities IC_{50} (nM)				Genuine predictions of IC_{50} (nM)			
Antagonist	Predicted	Actual	Ref.	Antagonist	Predicted	Actual	Ref.
3a	412	452	10a	**5a**	4.4	5.4	13g
3b	391	210	13a	**5b**	6.3	1.4	20d
3c	574	940	13a	**5c**	11	3.8	20a
3d	40.6	79	10a	**5d**	14	2	20a
3e	357	59	20a	**5e**	16	2	20a
3f	459	809	10a	**5f**	16	12	13g
3g	537	479	10a	**5g**	19	1.8	13a
3h	15.4	8.5	16b	**5h**	19	22	20a
3i	1127	539	16i	**2k**	48	8	16k
3j	1506	889	16i	**5i**	2.8	2.6	20i
3k	11.3	0.7	16a	**5j**	192	0.2	20p
3l	849	170	20b	**5k**	91	1.2	20h
3m	246	90	10b	**5l**	2.4	1.5	20k
3n	28.7	44	10n	**5m**	416	10 000	20j
3p	45.4	130	10a	**5n**	1.4	3	20k
3q	226	370	16b	**5p**	540	1200	20a
3r	323	210	20a	**5q**	14	120	20l
3s	494	940	16b	**5r**	1.7	12	20i
3t	43	620	10a	**5s**	2.9	5.6	20i
3u	31	50	10a	**5t**	1.5	3.6	20i
3v	140.6	370	16b	**5u**	46	60	13j
3w	14.1	20.3	16j	**5v**	16	14	13l
3x	7.5	20	16a	**5w**	178	360	20m
3y	22.7	100	20a	**5x**	105	55	20n
3z	177	85	10a	**5y**	7.9	2.9	20k
2a	11.9	1.3	16b	**5z**	0.6	0.8	20a
4a	14.1	4.1	16j	**6a**	5	51	20i
2g	6.9	3.2	16g	**2b**	34.9	2	13c
4b	17.6	18.3	16j	**2e**	0.7	0.1	13e
4c	15.1	23.2	16j	**2f**	87.0	8	13f
L158809	5.2	0.5	16a	**2h**	1.1	2	13h
4e	11.6	2	16b	**2i**	349.0	7	13i
4f	6.7	8.5	20d	**2j**	13.3	2	13j
4g	19.9	5.6	16c	**2l**	55.3	3	13c
4h	59.5	584	20e	**2m**	99.3	0.2	13l
4i	55.1	880	20c	**2p**	31.4	2	13l
4j	1.0	2.2	16e	ICI	26	12	
2d	0.5	0.2	16e	CIBA6D	362	600	
4k	67.3	101.6	16c	DUP753	31	24	
4l	29.3	54	16d				
4m	54.8	229.6	16c				
4n	30.9	8.7	16c				
4p	0.9	0.7	20f				
4q	0.5	0.6	20f				
2c	5.4	9.2	16d				
4r	6.6	20	20a				
4s	0.2	0.5	16e				
4t	14.2	26	16b				
4u	0.6	0.2	16e				
4v	20.8	54	20g				

and also are supported by the experimental SAR [31]. The region corresponding to the pyridine N of L-158809 has been implicated as contributing to AT_1 antagonism (Fig. 1a, **E**), illustrating that H-accepting groups (=O, =N–, COOH) will increase potency. Additionally, the field representations indicate that filling the 3-position of an imidazopyridine with steric bulk has a favorable effect on activity (Fig. 1a, **F**).

These results provide a consistent, *qualitative* picture of A-II antagonism, where the geometric constraints between functional groups must first match the distances found by search, while complementing the steric and electrostatic features of the receptor. The non-peptide antagonists considered here are compatible with this structural model. Of certain interest, then, is how the natural substrate compares to this predicted structure of the non-peptides. Several groups have attempted to overlay A-II (Asp-Arg-Val-Tyr-Ile-His-Pro-Phe) with non-peptide antagonists [3,32,36]. The implicit assumption in these models is that small-molecule and peptide antagonists bind at the same site on AT_1. Insofar that the SAR for the C-terminal portion of A-II tracks that of the small molecules, this is a reasonable working hypothesis. The confounding aspect of these comparisons, however, is that the bioactive conformation of A-II is not known. A popular conformational model places the C-terminal amino acids into a γ-turn [33]. Other models invoke hydrogen bonding between histidine, tyrosine, and the C-terminus [34]. Restricted peptide analogs have been prepared [35], but none of them either lock in or forbid these conformations. In fact, recent conformational analysis of peptide antagonists and agonists of A-II reveals that no single backbone geometry is mutually consistent between all restrained peptidyl analogs [37]. These findings suggest that the receptor identifies a peptidyl ligand predominantly through side-chain interactions, which could be mimicked successfully by small-molecule antagonists. The original peptide to non-peptide overlay proposed in the literature [3] equated **E** (Fig. 1a) to the C-terminus of A-II. As the small-molecule antagonists evolved, it became evident that the C-terminus of A-II maps to **A** [32]. Following this, Pierson and Freer performed a limited systematic search on A-II peptides and located the distance between the centroid of His^6 and the C-terminus to roughly 9 Å [32]. Their superpositions between A-II and DUP753 suggested that the bioactive conformation of DUP753 presents an 8.6 Å distance between the centroid of the tetrazole and the center of the imidazole. Our model, derived from systematic searching, identifies this distance as 8.5 Å, in close agreement with this independent determination. The intriguing similarity between two independently derived models presumes that the heterocycle of DUP753 mimics His^6 of A-II. However, it is not clear that the heterocycle ring of the small molecule mimics this side chain.

An illustration of our working superposition is shown in Fig. 11. The conformation of A-II used in these studies has been modeled by hand, to have ϕ,ψ angles generally consistent with the tolerated amino acid substitutions (or restrictions) on the activity of A-II. From this starting

TABLE 4
BACKBONE DIHEDRAL ANGLES (degrees) FOR ANGIOTENSIN-II

Residue	ϕ	ψ	Residue	ϕ	ψ
Asp^1	–	165	Ile^5	–61	–31
Arg^2	55	35	His^6	–117	134
Val^3	–84	–28	Pro^7	–81	66
Tyr^4	57	20	Phe^8	–80	–

point, the peptide was minimized using MM2X (intramolecular dielectric of 50 D), and the final ϕ,ψ angles are reported in Table 4. Our peptide conformation allows similar placement of the side chains from the C-terminal tetrapeptide segment of A-II, reported recently in the literature [38]. The C-terminal carboxylate is close to the tyrosine side chain. One insight arising from the superposition is the possibility that the 5-position of an imidazopyridine points toward the N-terminus of A-II, an observation consistent with existing SARs, which indicates that large substituents on the 5-position of the imidazo-pyridine ring do not adversely affect activity. As generally accepted, our mapping between peptide and non-peptide equates Ile^5 of A-II with the alkyl chain of L-158809, and the C-terminal phenylalanine (or isoleucine) with the terminal ring of the biphenyl. This model proposes that the heterocycle ring of the small molecule acts as a scaffold to ideally position substituents which mimic the 3- and 5-positions of the peptide. The pyridine N of the imidazopyridine ring is in the vicinity of an amide bond. It is clear from the superposition that A-II and the non-peptide antagonists are not of similar size, suggesting that not all the interactions made in one class would be present in the other. Mutational data on the AT_1 receptor could be extremely useful in mapping the precise interactions made by these ligands, and in identifying common binding motifs.

Should one be able to identify similarity between the 3D presentation of the small molecules and peptides? While there is no extensive mutational evidence for the A-II system, results obtained on the neurokinin receptor (NK_1) may be applicable, as it is also a G-protein-coupled receptor (GPCR) which binds peptides and non-peptides [40–44]. The NK_1 receptor has been the paradigm for advancing hypotheses of peptide–non-peptide interactions with GPCRs, and initial studies indicated that the epitopes for substance P and small molecules such as CP64325 were non-overlapping, in spite of the fact that the ligands exhibit competitive binding [40–43]. A recent site-directed mutagenesis study has identified at least one residue in NK_1 which potentially interacts with substance P and the hydroisoindole antagonist RP67580 [44]. Clearly, the story will become increasingly complex as more mutational data are collected, since 3D receptor models of NK_1 suggest that some of the sites which affect peptides but not small molecules are spatially close [41]. These results demonstrate that it is possible for peptides and non-peptides to share some receptor binding sites, even though not all the interactions will be maintained across series. By superposing regions with parallel structure–activity relationships, a hypothesis regarding which elements are likely to be overlapping and which are not can be generated. Taken in context with 3D receptor models, such superpositions could be very useful in the design and interpretation of site-directed mutagenesis studies. However, mutational data are not always straightforward to interpret: it has been suggested that some mutations alter global or local conformation of the receptor in a way which destroys the binding site for small molecules [42,43]. This should be kept in mind when interpreting experimental results as well as building 3D receptor models.

CONCLUSIONS

Systematic search has predicted a binding geometry for antagonists at the AT_1 receptor, by locating a three-dimensional arrangement of the defined pharmacophore points which is mutually consistent for all active analogs. This orientation map acts as an alignment rule to determine correspondence between assorted classes of antagonists, and has been shown to yield a good predictive model of activity as described by CoMFA. Our structural model also has been used

to generate overlays with A-II itself, in an effort to understand the requirements of the AT_1 receptor. While the pharmacophore map distances are reported with the precision used in their derivation, it is unlikely that such stringent tolerances are actually necessary for receptor *recognition*. However, these distances are required of the most potent analogs which bind to the same pharmacophoric elements.

This work uses existing methods in concert to understand the conformational restraints on non-peptidyl antagonists of A-II. Even with a literature precedent for successful application of these techniques [8], it was not clear at the inception of this study that enough restraints had been imposed to propose a unique receptor-bound geometry. Further, CoMFA has generally been applied within a structural class, rather than across several series. We hope not to be too cavalier in advancing the successes of an obviously simplistic physical model: our CoMFA neglects energy, entropy and solvation effects in its calculation of IC_{50} values. In addition, the choice of search parameters has possibly over-reduced the number of viable solutions, as no change in geometry is permitted when mapping conformational space. Moreover, the tolerance between mapped distances must be identical, implying a very rigid binding geometry with equivalent stringency of recognition between pharmacophoric elements. Recent work, outlining an improved and rapid PLS cross-validation approach, makes it possible to consider evaluating multiple structural alignments [39]. This advance will allow more conformational models and larger sets of CoMFA descriptors (hydrophobicity, H-donor) to be considered. However, the coupling of these two methods (search and CoMFA) improves the credibility of each. The apparent success of this study indicates that these methods are applicable to highly complicated problems, and can yield useful information when a crystal structure of the receptor environment is lacking. The structural hypothesis can now be used, in conjunction with models of the A-II receptor, to further enlighten an area in which very little structural data are available, but are eagerly awaited.

ACKNOWLEDGEMENTS

The authors would like to thank Dr. J. Chris Culberson of Merck Research Laboratories for modifications to the visualization program C_VIEW which allowed CoMFA fields to be viewed (unpublished results, 1992).

REFERENCES

1 Vallotton, M.B., Trends Pharmacol. Sci., 8 (1987) 69.
2 a. Bovy, P.R. and Baline, E.H., Curr. Cardiovasc. Patents, 1 (1989) 2044.
b. Turker, R.K., Hall, M.M., Yamamoto, M., Sweet, C.S. and Bumpus, F.M., Science, 177 (1972) 1203.
c. Hall, M.M., Khosla, M.C., Kairallah, P. and Bumpus, F.M., J. Pharmacol. Exp. Ther., 188 (1974) 222.
3 Duncia, J.V., Chiu, A.T., Carini, D.J., Gregory, G.B., Johnson, A.L., Price, W.A., Wells, G.J., Wong, P.C., Calabrese, J.C. and Timmermans, P.B.M.W.M., J. Med. Chem., 33 (1990) 1312.
4 a. Christen, Y., Waeber, B., Nussberger, J., Porchet, M., Lee, R.J., Maggon, K., Timmermans, P.B.M.W. and Brunner, H.R., J. Hypertens., 8 (1990) S16.
b. Christen, Y., Waeber, B., Nussberger, J., Porchet, M., Borland, R.M., Lee, R.J., Maggon, K., Shum, L., Timmermans, P.B.M.W. and Brunner, H.R., Circulation, 83 (1991) 1333.
5 Underwood, D.J., Strader, C., Rivero, R., Patchett, A.A., Greenlee, W.J. and Prendergast, K., (1994) manuscript in preparation.
6 Mayer, D., Naylor, C.B., Motoc, I. and Marshall, G.R., J. Comput.-Aided Mol. Design, 1 (1987) 3.

7 Cramer III, R.D., Patterson, D.E. and Bunce, J.D., J. Am. Chem. Soc., 110 (1988) 5959.

8 DePriest, S.A., Mayer, D., Naylor, C.B. and Marshall, G.R., J. Am. Chem. Soc., 115 (1993) 5372.

9 a. Duncia, J.V., Carini, D.J., Chiu, A.T., Johnson, A.L., Price, W.A., Wong, P.C., Wexler, R.R. and Timmermans, P.B.M.W., Med. Res. Rev., 12 (1992) 149.

b. Lin, H., Rampersaud, A., Zimmerman, K., Steinberg, M.I. and Boyd, D.B., J. Med. Chem., 35 (1992) 2658.

10 a. Chakravarty, P.K., Camara, V.J., Chen, A., Marcin, L.M., Greenlee, W.J., Patchett, A.A., Chang, R.S., Lotti, V. and Siegl, P.K.S., 200th National Meeting of the American Chemical Society, Washington, DC, August 26–31, 1990.

b. Rivero, R., Merck Research Laboratories, unpublished work, 1989.

11 SYBYL, Version 5.2, TRIPOS Associates, St. Louis, MO, 1989.

12 Ohta, M. and Koga, H., J. Med. Chem., 34 (1991) 131.

13 a. Mantlo, N.B., Chakravarty, P.K., Ondeyka, D.L., Siegl, P.K.S., Chang, R.S., Lotti, V.J., Faust, K.A., Chen, T.-B., Schorn, T.W., Sweet, C.S., Emmert, S.E., Patchett, A.A. and Greenlee, W.J., J. Med. Chem., 34 (1991) 2919.

b. Allen, E.E., deLaszlo, S.E., Huang, S.X., Quagliato, C.S., Greenlee, W.J., Chen, R.T., Faust, K.A. and Lotti, V.J., Bioorg. Med. Chem. Lett., 3 (1993) 1293.

c. Dhanoa, D., Bagley, S.W., Chang, R.S.L., Lotti, V.J., Siegl, P.K.S., Patchett, A.A. and Greenlee, W.J., 204th National Meeting of the American Chemical Society, Washington, DC, August 23–28, 1992.

d. Greenlee, W.J., Johnston, D.B.R. and MacCoss, M., U.S. Patent No. 5,157,040, 1992.

e. Naylor, E.M., Chakravarty, P.K., Chen, A., Strelitz, R.A., Chang, R.S., Chen, T.B., Faust, K.A., Lotti, V.J., Kivlighn, S.D., Zingaro, G.J., Schorn, T.W., Siegl, P.K.S., Patchett, A.A. and Greenlee, W.J., 206th National Meeting of the American Chemical Society, Chicago, IL, August 22–27, 1993.

f. Fitch, K.J., Walsh, T.F., Patchett, A.A., Chang, R.S.L. and Greenlee, W.J., 205th National Meeting of the American Chemical Society, Denver, CO, March 28 – April 2, 1993.

g. Ondeyka, D.L., Mantlo, N.B., Chakravarty, P.K., Chen, A., Camara, V.J., Chang, R.S.L., Lotti, V.J., Siegl, P.K.S., Patchett, A.A. and Greenlee, W.J., Joint Central-Great Lakes Regional Meeting of the American Chemical Society, Indianapolis, IN, May 31, 1991.

h. Kevin, N.J., Rivero, R.A., Greenlee, W.J. and Chang, R.S., 205th National Meeting of the American Chemical Society, Denver, CO, March 28 – April 2, 1993.

i. Ashton, W.T., Cantone, C.L., Chang, L.L., Hutchins, S.M., Strelitz, R.A., MacCoss, M., Chang, R.S.L., Lotti, V.J., Faust, K.A., Chen, T.-B., Bunting, P., Schorn, T.W., Kivlighn, S.D. and Siegl, P.K.S., J. Med. Chem., 36 (1993) 591.

j. Chang, L.L., Ashton, W.T., Flanagan, K.L., Strelitz, R.A., MacCoss, M., Greenlee, W.J., Chang, R.S.L., Lotti, V.J., Faust, K.A., Chen, T.B., Bunting, P., Zingaro, G.J., Kivlighn, S.D. and Siegl, P.K.S., J. Med. Chem., 36 (1993) 2558.

k. Allen, E., Merck Research Laboratories, unpublished work, 1989.

l. Allen, E.E., Greenlee, W.J., Chakravarty, P.K., Patchett, A.A. and Walsh, T.F., U.S. Patent No. 5,100,897, 1992.

14 OPTIMOL contains the MM2X force field, which differs from MM2 principally in that electrostatic interactions take place between atom-centered charges. The atomic charges (q) are derived from the bond dipole moments (μ): $q = (1/4.803) \Sigma_i \mu_i r_{0i}$. Here, r_0 is the reference bond length. This is the only difference in the functional form of MM2X with respect to MM2 [15]. Parameters for the nonbond out of plane and stretch–bend interactions are taken directly from MM2. MM2X does not use lone pairs on aliphatic amines, ether oxygens, and carboxylic acid and ester oxygens, and any parameterization differences are primarily due to the need to make up this difference. OPTIMOL has been developed at Merck Research Laboratories by T.A. Halgren and other members of the Molecular Systems Department [16].

15 Allinger, N.L., J. Am. Chem. Soc., 99 (1977) 8127.

16 Halgren, T.A., J. Am. Chem. Soc., 114 (1992) 7827.

17 The MM2 force field, as supplied with Batchmin (Still, W.C., Mohamadi, F., Richards, N.J.G., Guida, W.C., Liskamp, R., Lipton, M., Caufield, C., Chang, G. and Hendrickson, T., MACROMODEL, Version 4.0, Department of Chemistry, Columbia University, New York, NY), was used with the following supplemental parameters: N2*N2 bonds were set at 1.326 Å and 7.72 mdyn/Å^2; N2*C2*N2 angles were set at 128° and 0.96 mdyn/rad^2; *N2* angles were set at 123° and 0.7 mdyn/rad^2; and C2*C2*C3*N2 and O3*C2*C3*N2 torsions both have their V2 terms set at 0.7 kcal/mol. C2*S1*N2*C3 torsions were set at V1 = 2.805 kcal/mol, V2 = –1.133 kcal/mol and V3 = –0.621 kcal/mol,

while N3*S1*N2A*C3 torsions were set at V1 = 0 kcal/mol, V2 = 1.133 kcal/mol, and V3 = 0.621 kcal/mol. An external angle description for azinoid and pyridinoid fragments (N2*AA*AA*AA*AA*, N2*AA*AA*AA*AA*AA*) was added as 122.5°, with a force constant of 0.5 mdyn/Å^2.

18 SYBYL, Version 5.32, TRIPOS Associates, St. Louis, MO, 1990.

19 Dewar, M.J.S. and Thiel, W., J. Am. Chem. Soc., 99 (1977) 4899.

20 a. Chakravarty, P.K., Greenlee, W.J., Mantlo, N.B., Patchett, A.A. and Walsh, T.F., European Patent Application 400,974, 1990.
b. Chakravarty, P.K., Patchett, A.A., Camara, V.J., Walsh, T.F. and Greenlee, W.J., European Patent Application 400,835, 1990.
c. Allen, E.E., Greenlee, W.J., MacCoss, M. and Patchett, A.A., U.S. Patent No. 5,166,206, 1992.
d. Mantlo, N.B., Ondeyka, D., Chang, R.S.L., Lotti, V.J., Kivlighn, S.D., Siegl, P.K.S., Patchett, A.A. and Greenlee, W.J., 202nd National Meeting of the American Chemical Society, New York, NY, September 5–10, 1991.
e. Bagley, S., Greenlee, W.J., Dhanoa, D.S. and Patchett, A.A., U.S. Patent No. 5,175,164, 1992.
f. Allen, E.E., Huang, S.X., Chang, R.S.L., Lotti, V.J., Siegl, P.K.S., Patchett, A.A. and Greenlee, W.J., 202nd National Meeting of the American Chemical Society, New York, NY, August 25–30, 1991.
g. Patchett, A.A., Mantlo N.B. and Greenlee, W.J., U.S. Patent No. 5,124,335, 1992.
h. Glinka, T.W., deLaszlo, S.E., Siegl, P.K.S., Chang, R.S.L., Kivlighn, S.D., Schorn, T.S., Faust, K.A., Chen, T.B., Zingaro, G.J., Lotti, V.J. and Greenlee, W.J., Bioorg. Med. Chem. Lett., 4 (1994) 81.
i. Chakravarty, P.K., Strelitz, R.A., Chen, T.-B., Chang, R.S.L., Lotti, V.J., Zingaro, G.J., Schorn, T.W., Kivlighn, S.D., Siegl, P.K.S., Patchett, A.A. and Greenlee, W.J., Bioorg. Med. Chem. Lett., 4 (1994) 75.
j. Chakravarty, P.K., Merck Research Laboratories, unpublished work, 1990.
k. Allen, E., deLaszlo, S.E., Greenlee, W.J., Patchett, A.A., Chakravarty, P.K. and Walsh, T.F., European Patent Application EP-411,766, 1990.
l. Greenlee, W.J., Johnston, D.B.R., MacCoss, M., Mantlo, N.B., Patchett, A.A., Chakravarty, P.K. and Walsh, T.F., U.S. Patent No. 5,164,407, 1992.
m. Kevin, N.J., Rivero, R.A. and Greenlee, W.J., 202nd National Meeting of the American Chemical Society, New York, NY, August 25–30, 1991.
n. Walsh, T., Merck Research Laboratories, unpublished work, 1989.
o. Ashton, W.T., Hutchins, S.M., Greenlee, W.J., Doss, G.A., Chang, R.S.L., Lotti, V.J., Faust, K.A., Chen, T.-B., Zingaro, G.J., Kivlighn, S.D. and Siegl, P.K.S., J. Med. Chem., 36 (1993) 3595.

21 Kearsley, S.K. and Smith, G.H., Tetrahedron Comput. Methodol., 3 (1990) 615.

22 Adams, K., Merck Research Laboratories, unpublished work, 1991.

23 a. Bradbury, R.H., Allot, C.P., Dennis, M., Fisher, E., Major, J.S., Masek, B.B., Oldham, A.A., Pearce, R.J., Rankine, N., Revill, J.M., Roberts, D.A. and Russell, S.T., J. Med. Chem., 35 (1992) 4027.
b. Masek, B.B., Merchant, A. and Matthew, J.B., J. Med. Chem., 36 (1993) 1230.
c. Perkins, T.D.J. and Dean, P.M., J. Comput.-Aided Mol. Design, 7 (1993) 155.
d. Thomas, A.P., Allott, C.P., Gibson, K.H., Major, J.S., Masek, B.B., Oldham, A.A., Ratcliffe, A.H., Roberts, D.A., Russell, S.T. and Thomason, D.A., J. Med. Chem., 35 (1992) 877.

24 Martin, Y.C., Bures, M.G., Danaher, E.A., DeLazzer, J., Lico, I. and Pavlik, P.A., J. Comput.-Aided Mol. Design, 7 (1993) 83.

25 a. Crippen, G. and Havel, T.F., Acta Crystallogr., A34 (1987) 282.
b. DGEOM, written by J.D. Andose, Merck Research Laboratories, 1992.

26 Buehlmayer, P., Criscione, L., Fuhrer, W., Furet, P., diGaspous, M., Sturtz, S. and Whitebread, S., J. Med. Chem., 34 (1991) 3105.

27 Wong, P.C., Price Jr., W.A., Chiu, A.T., Thoolen, M.J.M.C., Duncia, J.V., Johnson, A.L. and Timmermans, P.B.M.W.M., Hypertension, 13 (1989) 489.

28 Chiu, A.T., McCall, D.E., Price, W.A., Wong, P.C., Carini, D.J., Duncia, J.V., Wexler, R.R., Yoo, S.E., Johnson, A.L. and Timmermans, P.B.M.W.M., J. Pharmacol. Exp. Ther., 252 (1990) 711.

29 Bradbury, R.H., Allott, C.P., Girdwood, J.A., Kenny, P.W., Major, J., Oldham, A.A., Ratcliffe, A.H., Rivett, J.E., Roberts, D.A. and Robins, P.J., J. Med. Chem., 36 (1993) 1245.

30 Kearsley, S.K., Sallamack, S., Sheridan, R.P., Fluder, E.M. and Andose, J.D., J. Chem. Inf. Comput. Sci., in press.

31 Mantlo, N.B., Chakravarty, P.K., Ondeyka, D.L., Siegl, P.K.S., Chang, R.S., Lotti, V.S., Faust, K.A., Chen, T.B.,

Schorn, T.W., Sweet, C.S., Emment, S.E., Patchett, A.A. and Greenlee, W.J., J. Med. Chem., 34 (1990) 2919.
32 a. Weinstock, J., Keenan, R.M., Samanen, J., Hempel, J., Finkelstein, J.A., Franz, R.G., Gaitanopolos, D.E., Girard, G.R., Gleason, J.G., Hill, D.T., Morgan, T.M., Peishoff, C.E., Aiyar, A., Brooks, D.P., Fredrickson, T.A., Ohlstein, E.H., Ruffalo, R.R., Stank, E.J., Sulpizio, A.C., Weidley, E.F. and Edwards, R.M., J. Med. Chem., 34 (1991) 1514.
b. Samanen, J.M., Peishoff, C.E., Keenan, R.M. and Weinstock, J., Bioorg. Med. Chem. Lett., 3 (1993) 909.
33 Smeby, R.R. and Fermandjian, S., In Weinstein, B. (Ed.) Chemistry and Biochemistry of Amino Acids, Peptides, and Proteins, Marcel Dekker, New York, NY, 1978, pp. 117–162.
34 a. Moore, G.J., Int. J. Pept. Protein Res., 26 (1985) 469.
b. Turner, R.J., Matsoukas, J.M. and Moore, G.J., Biochem. Biol. Acta, 1065 (1991) 21.
35 a. Sugg, E.E., Dolan, C.A., Patchett, A.A., Chang, R.S.L., Faust, K.A. and Lotti, V., In Rivier, J.E. and Marshall, G.R. (Eds.) Peptides: Chemistry, Structure and Biology (Proceedings of the 11th American Peptide Symposium), ESCOM, Leiden, 1990, pp. 305–306.
b. Kataoka, T., Beuser, D.D., Clark, J.D., Yodo, M. and Marshall, G.R., Biopolymers, 32 (1992) 1519.
c. Samanen, J., Cash, T., Narindray, D. and Brandeis, E., J. Med. Chem., 34 (1992) 3036.
d. Juvvadi, P., Dooley, D.J., Humblet, C.C., Lu, G.H., Lunney, E.A., Panek, R.L., Skeean, R. and Marshall, G.R., Int. J. Pept. Protein Res., 40 (1992) 163.
e. Spear, K.L., Brown, M.S., Reinhard, E.J., McMahon, E.G., Olins, G.M., Palema, M.A. and Patta, D.R., J. Med. Chem., 33 (1990) 1935.
36 Pierson, M.E. and Freer, R.J., Pept. Res., 5 (1992) 102.
37 Plucinska, K., Kataoka, T., Yodo, M., Cody, W.L., He, J.X., Humblet, C., Lu, G.H., Lunney, E., Major, T.C., Panek, R.L., Schelkun, P., Skeean, R. and Marshall, G.R., J. Med. Chem., 36 (1993) 1902.
38 Nikiforovich, G.V. and Marshall, G.R., Biochem. Biophys. Res. Commun., 195 (1993) 222.
39 Bush, B.L. and Nachbar, R.B., J. Comput.-Aided Mol. Design, 7 (1993) 587.
40 Gether, U., Johansen, T.E., Snider, R.M., Lowe, J.A., Nakanishi, S. and Schwartz, T.W., Nature, 352 (1993) 345.
41 Casciere, M., Macleod, A.M., Underwood, D., Shiao, L., Ber, E., Sadowski, S., Yu, H., Merchant, K.J., Swain, C.J., Strader, C.D. and Fong, T.M., J. Biol. Chem., 269 (1994) 6587.
42 Sachais, B., Snider, R.M., Lowe, J.A. and Krause, J.E., J. Biol. Chem., 268 (1992) 2319.
43 Jensen, C.J., Gerard, N.P., Schwartz, T.W. and Gether, U., Mol. Pharmacol., 45 (1994) 294.
44 Huang, R.C., Yu, H., Strader, C.D. and Fong, T.M., Biochemistry, 33 (1994) 3007.